Effect of crystallization on apatite-layer formation of bioactive glass 45S5

Oscar Peitl Filho,[1] Guy P. LaTorre,[2] and Larry L. Hench[2,*]
[1]*São Carlos Federal University, São Carlos, São Paulo, Brazil;* [2]*Advanced Materials Research Center, University of Florida, Gainesville, Florida*

The bioactive glass 45S5 was crystallized to 8–100 vol % of crystals by thermal treatments from 550–680°C. The microstructure of the glass-ceramics had a very uniform crystal size, ranging from 8 to 20 μm. Fourier-transform infrared (FTIR) spectroscopy was used to determine the rate of hydroxycarbonate apatite (HCA) formation that occurs on bioactive glass and glass-ceramic implants when exposed to simulated body fluid (SBF) solutions. Crystallization did not inhibit development of a crystalline HCA layer, but the onset time of crystallization increased from 10 h for the parent glass to 22 h for 100% crystallized glass-ceramic. The rate of surface reactions was slower when the percentage of crystallization was $\geq$ 60%. © 1996 John Wiley & Sons, Inc.

INTRODUCTION

A common characteristic of bioactive glasses and glass-ceramics is the formation of a biologically active apatite layer which provides the bonding with bone.[1] Many efforts have been made to understand the formation of hydroxycarbonate apatite (HCA) on bioactive glass and glass-ceramics.[1–7] Studies have shown that 12 stages of reactions occur on the material–tissue interface, as summarized in Table I. Five of the reaction stages occur on the material side of the interface. These stages are most rapid for implants with the highest level of bioactivity.[2] Reaction stages 6–12 occur on the tissue side of the interface, and stages 6 and 7 probably overlap with stages 3–5. However, a full understanding of the mechanisms of stages 6–8 has not been reached.

Quantitative data for the rates of stages 1–5 use Fourier-transform infrared (FTIR) with a diffuse reflection stage, which is a very sensitive method for detection of crystallization of HCA (stage 5), as previously demonstrated in both tris buffer and simulated body fluids (SBFs).[3,4] Kokubo et al.[5] showed that a tris-buffer solution did not produce a HCA layer on bone-bonding apatite/wollastonite (A/W) glass-ceramic. However, exposure of A/W glass-ceramic to a SBF that contained ions in concentration similar to those of the human body produced a polycrystalline HCA layer.[5]

Li et al.[6] showed that when a bioactive glass containing (in wt %) SiO_2 48, P_2O_5 9.5, Na_2O 20, and CaO 22.5 is transformed into a glass-ceramic the formation of the surface apatite layer in tris-buffer solution depends on the relative amount of residual glassy phase in the glass-ceramic. They showed that a glass-ceramic with 5% or less of residual glassy phase exhibited no formation of a surface HCA layer, even when exposed to SBF solutions.

A few studies[6–9] have examined the effect of crystallization of bioactive glasses on kinetics of HCA formation; however, there is sparse data on the effect of volume fraction of the crystal phase on the surface reaction rates. Thus, the objective of this work was to quantify the effect of crystallization of a highly bioactive glass (45S5 Bioglass®) on HCA-layer formation (stage 5) *in vitro*.

EXPERIMENTAL

High-purity silica and reagent-grade calcium, sodium carbonate, and sodium phosphate were weighed and mixed to obtain 45S5 glass (45 SiO_2, 24.5 CaO, 24.5 Na_2O, 6.0 P_2O_5 in wt %). The glass was melted in a Pt crucible for 4 h at 1330°C, and poured into graphite molds to form 8-mm × 30-mm cylinders.

*To whom correspondence should be addressed at AMRC, University of Florida, One Progress Blvd., Box 14, Alachua, FL 32615.

Journal of Biomedical Materials Research, Vol. 30, 509–514 (1996)

CCC 0021-9304/96/040509-06

TABLE I
Sequence of Interfacial Reactions Involved in Forming a Bond between Tissue and Bioactive Ceramics

Log Time (h)		Surface Reaction Stages
100	12	Proliferation of bone
	11	Crystallization of matrix
	10	Generation of matrix
	9	Differentiation of stem cells
20	8	Attachment of osteoblast stem cells
	7	Action of macrophages
10	6	Adsorption of biological moieties in HCA layer
2	5	Crystallization of hydroxyl carbonate apatite (HCA)
1	4	Adsorption of amorphous Ca + PO_4 + CO_3
	3	Polycondensation of SiOH + SiOH → Si-O-Si
	1 & 2	Formation of SiOH bonds and release of $Si(OH)_4$
		Bioactive glass

After annealing for 8 h at 460°C the cylinders were cut into disks. The disks were heat treated for nucleation at 550°C for 150 h, and then heated to 680°C at different times from 113 to 66 min for crystallization. The crystal phase grown in the glass-ceramic was $Na_2Ca_2Si_3O_9$ (1N2C3S), as determined with x-ray diffraction (XRD). The main XRD peaks of the crystal phase are shown in Figure 1. The Miller hk ℓ indices of the crystals match closely the 2θ location and relative intensity of the 1N2C3S phase, as determined by x-ray card 22.1455. The glass-ceramic disks were polished with 320-, 600-, and 1200-grit SiC and 1 μm cerium oxide, and then etched with an HF solution (0.05%) for 10 s. The quantitative microstructure of the glass-ceramic specimen was investigated with an optical microscope using point-counting stereology methods.

The SBF was prepared mixing sodium chloride, sodium bicarbonate, potassium chloride, calcium chloride, dibasic potassium phosphate, and magnesium chloride in deionized water.[5] The concentrations used are listed in Table II.

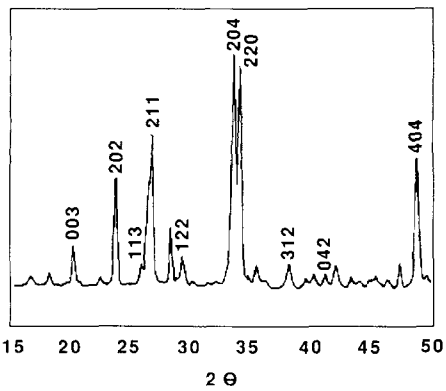

Figure 1. XRD spectra of glass-ceramic with 50% crystallinity.

TABLE II
Ion Concentration (m*M*) of SBF and Human Plasma

Ion	SBF-K9	Blood Plasma
Na^+	142.0	142.0
K^+	5.0	5.0
Mg^{2+}	1.5	1.5
Ca^{2+}	2.5	2.5
Cl^-	147.8	103.0
HCO_3^-	4.2	27.0
HPO_4^{2-}	1.0	1.0
SO_4^{2-}	0.5	0.5

Fourier-transform infrared spectroscopy was performed on the glass and glass-ceramic disks before and after exposure to SBF at 37°C solution using a Nicolet model 20SXB spectrometer with a diffuse-reflectance stage. Spectra were obtained between 1400 and 400 cm^{-1} at 2 cm^{-1} resolution using a triglycerin sulfate (TGS) detector. Multiple samples (n = 3–5) were tested and analyzed under identical conditions. The range of times required to form a crystalline HCA layer (stage 5 in Table I) in SBF are reported.

RESULTS

The infrared spectral-peak assignments for the molecular vibrations observed have been discussed previously.[10,11] The regions of special interest are listed in Table III. Figure 2 presents the optical microstructures of the glass-ceramics for several volume percentages of crystallization (α), α = 8%, 36%, 60%, 87%, and 100%, respectively. The microstructures obtained by homogeneous nucleation are very uniform, and grain sizes range from 8 μm (α = 8%) to 25 μm (α = 100%).

TABLE III
Infrared Frequencies for Functional Groups on a Bioactive Glass Surface before and after SBF Reaction

Wavenumber (cm^{-1})	Vibrational Mode	
1350–1080	P=O	stretch
1250–1100	P = O	associated
940–860	Si-O-Si	stretch
890–800	C-O	stretch
1175–710	Si-O-Si	tetrahedral
610–600	P-O	bend crystal
560–550	P-O	bend amorphous
530–515	P-O	bend crystal
540–4515	Si-O-Si	bend

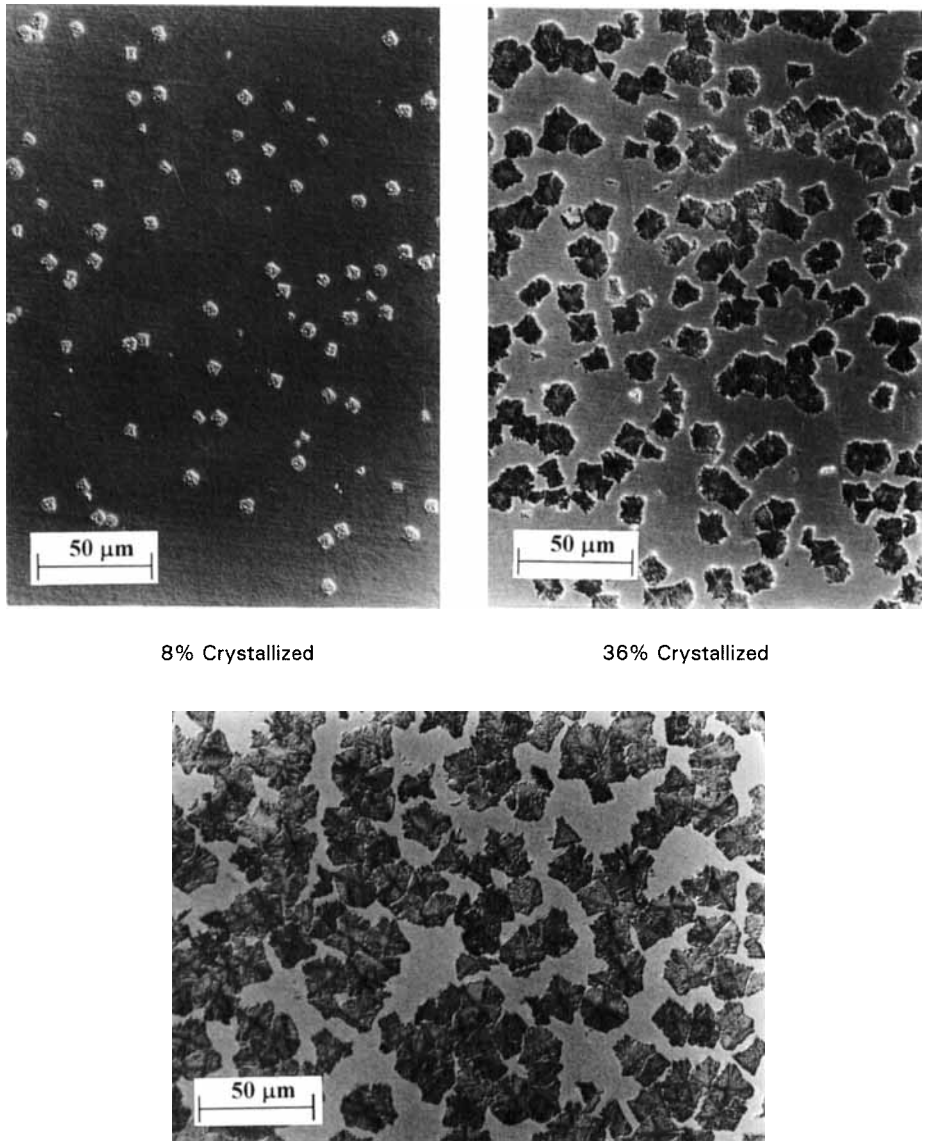

8% Crystallized

36% Crystallized

60% Crystallized

Figure 2. Glass-ceramic micrographs with 8%, 36%, 60%, 87%, and 100% crystallization, respectively. (Continued on next page.)

The FTIR spectra of the parent glass and the glass-ceramics before exposure to SBF and after 20 and 40 h reaction are shown in Figures 3, 4, and 5, respectively. The most noticeable changes in the IR spectra in Figure 3 relative to the unreacted amorphous glass are seen between 700 cm^{-1} and 400 cm^{-1}. Above α = 36% several new peaks emerge at 460 cm^{-1}, 575 cm^{-1}, and 650 cm^{-1}, which are attributed to vibrational modes of the developing crystal phase.

Specimens exposed to SBF solution for 20 h are seen in Figure 4. The glass-ceramics with more than 60% crystallinity develop only an amorphous calcium-phosphate film (stage 4) after 20 h exposure. However glass-ceramics with less than 60% crystallinity show crystalline HCA formation at the same time period. After 40 h exposure to SBF (Fig. 5) the glass-ceramics with > 60% crystallinity also exhibited fully developed crystalline HCA layers. In both Figures 4 and 5 there is an absence of most peaks associated with the crystal phase of the glass-ceramic; all peaks shown are due to either the amorphous calcium-phosphate layer or crystalline phases of HCA. A summary of the effects of volume percent of crystal phase on onset time of HCA crystallization is shown in Figure 6. The mean and ± one standard deviation of the onset time are indicated.

DISCUSSION

Previous efforts to improve the mechanical properties of bioactive glasses while maintaining bioactivity have been investigated, through controlled crystal

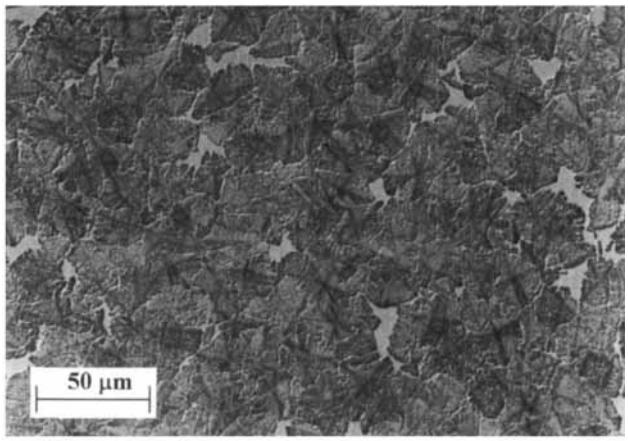

87% Crystallized

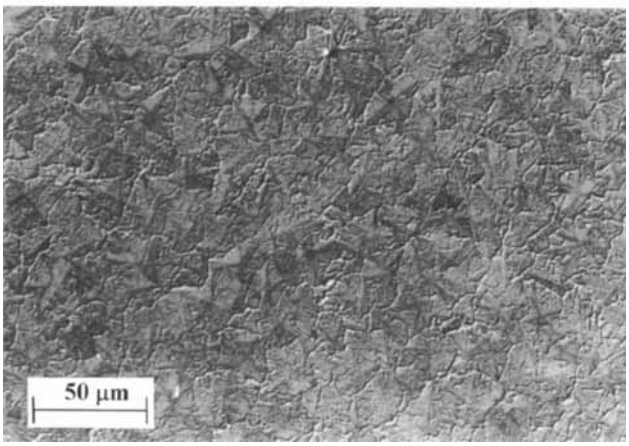

100% Crystallized

Figure 2. Continued.

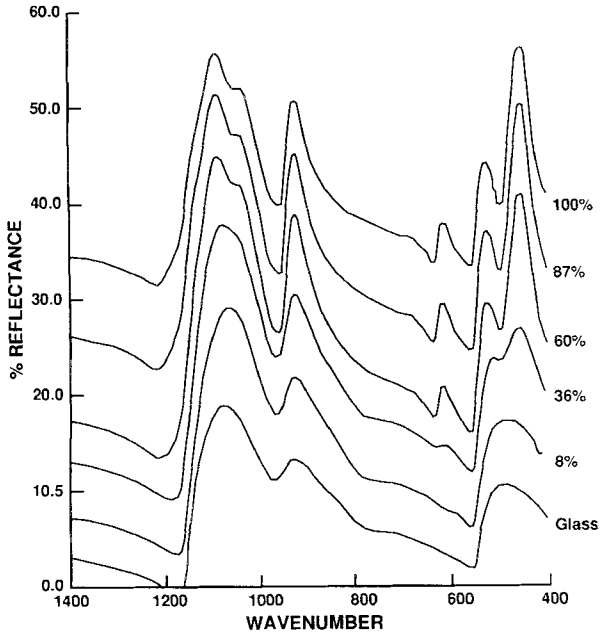

Figure 3. FTIR spectra of 45S5 bioactive glass and glass-ceramics with 8–100% crystallization, prior to reaction with SBF solution.

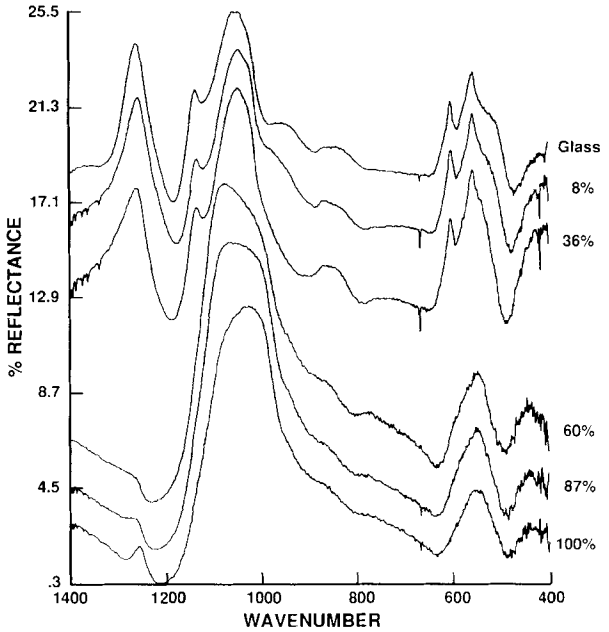

Figure 4. FTIR spectra of bioactive glass and glass-ceramics after 20 h exposure in SBF.

growth, by reinforcement by SiC whiskers, and by addition of tetragonal zirconia.[12,13] However, there is little correlation of the bioactivity of the two phase materials as a function of percent crystallinity. Bioactivity studies conducted on glass-ceramics with a composition similar to those in our system, in tris buffer,[6] indicated that no apatite was formed on glass samples with 89% crystallinity when reacted for even as long as 140 h.

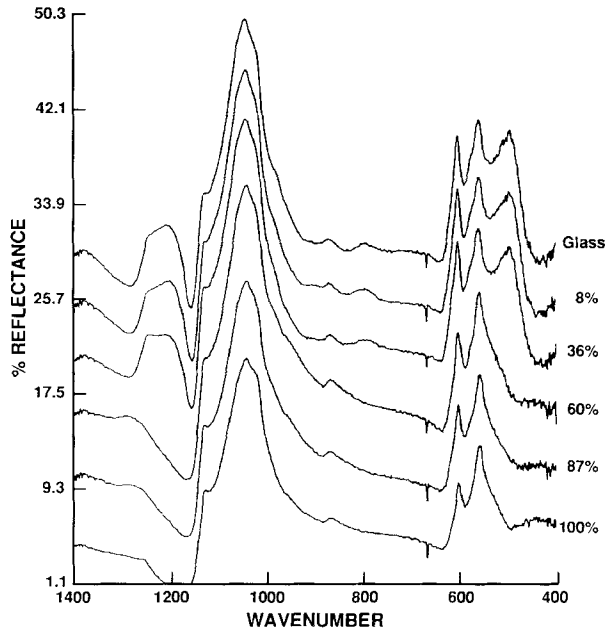

Figure 5. FTIR spectra of glass and glass-ceramics after 40 h exposure in SBF.

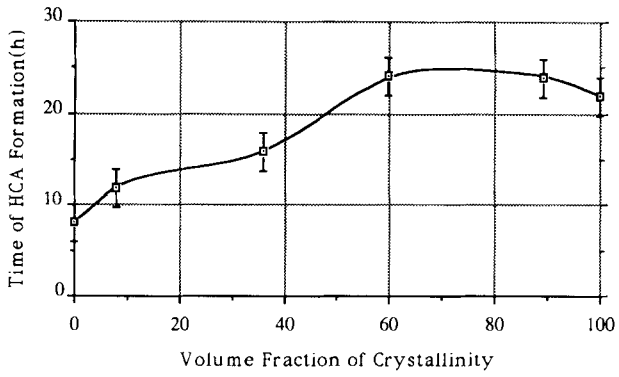

Figure 6. Onset time of HCA formation, stage 5, with percent crystallization of the bioactive glass-ceramics.

Similar studies with A/W glass-ceramic in SBF solution[5] indicate that apatite was formed only after 7 days reaction time but with no reference to the amount of residual glassy phase present. In contrast to these findings, the work presented here indicates that there is no compromise in bioactivity for the 45S5 glass-ceramic system with even 100% crystallinity.

After 20 h exposure to SBF solution (Fig. 4) the glass-ceramics with $\alpha > 60\%$ crystallinity show development of a well established amorphous calcium-phosphate layer with a peak due to P-O vibrations at 580 cm^{-1}. The glass-ceramics with $\alpha < 60\%$ indicate the presence of a crystalline HCA layer at 20 h, with dual peaks due to P-O modes at 560 cm^{-1} and 602 cm^{-1}. The results also show that as the percent crystallinity decreases from 36% to the amorphous glass the thickness of the crystalline apatite layer increases, as noted by the relative intensity of the P-O modes to the Si-O-Si rocking vibration. By 40 h exposure all spectra indicate the absence of the Si-O-Si mode, indicating a thick, well established crystalline HCA layer.

Although all the glass-ceramics studied, from 8% to 100% crystallinity, formed crystalline HCA when exposed to a SBF solution, the onset time of HCA crystallization was shifted from 10 h for the amorphous glass to 22–25 h for the 60–100% crystalline material. The increase in onset time for HCA increased with percentage crystallinity up to 60%, at which point the onset time remained relatively constant. The formation of a crystalline HCA layer depends on several variables, including the rate of ion exchange, hydroxylation of the glass surface, and pH and ion concentration of the solution.[4–11] The effect of crystallinity on HCA onset time up to 60% crystalinity appears to be related to the connectivity of the residual glassy phase, which controls the rate of ion exchange and silanol formation. However, because of the complex nature of the surface reactions it is difficult to determine the specific variables responsible for the constant onset time of HCA crystallization observed for the glass-ceramics at and above 60% crystallization.

CONCLUSIONS

The results show that 45S5 glass-ceramics with a crystal phase from 8% to 100% maintained their bioactivity when tested in an SBF solution. There is no loss in bioactivity with crystallinity up to 100%, contrary to results from other investigators with glasses of related compositions. The reaction rate observed in the 45S5 glass-ceramic was found to be up to seven times faster than that reported for A/W glass-ceramics with respect to the formation of crystalline HCA (stage 5).

One of the authors (O.P.F.) gratefully acknowledges support of the Brazilian government Conselho Nacional de Desenvolvimento Cientifico Tecnológico (CNPq) Secretaria de Ciência e Tecnologia. Two authors (G.L. and L.L.H.) acknowledge support of Air Force Office of Scientific Research Grant F49620-92-J-0351.

References

1. L. L. Hench, "Bioceramics: From concept to clinic," *J. Am. Ceram. Soc.*, **74,** 1487–1510 (1991).
2. L. L. Hench, "Bioactive ceramics," in *Bioceramics: Materials Characteristics versus in vivo Behavior, Vol. 523,* P. Ducheyne and J. E. Lemons (eds.), Annals of the New York Academy of Sciences, 1988, pp. 54–71.
3. L. L. Hench and G. P. LaTorre, "Reaction kinetics of bioactive ceramics, part IV: Effect of glass and solution composition," in *Bioceramics 5,* T. Yamamuro, T. Kokubo, and T. Nakamura (eds.), Kobonshi Kankokai, Inc., Kyoto, Japan, 1992 pp. 67–74.
4. M. R. Filgueiras, G. P. LaTorre, and L. L. Hench, "Solution effects on the surface reactions of a bioactive glass," *J. Biomed. Mater. Res.*, **27,** 445–453 (1993).
5. T. Kokubo, H. Kushitani, S. Sakka, T. Kitsugi, and T. Yamamuro, "Solutions able to reproduce *in vivo* surface-structure changes in bioactive glass-ceramic A-W," *J. Biomed. Mater. Res.*, **24,** 721–734 (1990).
6. P. Li, Q. Yang, F. Zhang, and T. Kokubo, "The effect of residual glassy phase in a bioactive glass-ceramic on the formation of its surface apatite layer *in vitro*," *J. Biomed. Mater. Res.*, **3,** 452–456 (1992).
7. F. H. Lin and M. H. Hon, "A study on bioglass ceramics in the Na_2O-CaO-SiO_2-P_2O_5 system," *J. Mater. Sci.*, **23,** 4295–4299 (1988).
8. L. L. Hench, "Bioactive glasses and glass-ceramics: A perspective," in *Handbook of Bioactive Ceramics, Vol. I,* T. Yamamuro, L. L. Hench, and J. Wilson (eds.), (CRC Press, Boca Raton, FL, 1990, pp. 7–23.
9. L. L. Hench, "Characterization of bioceramics," in *Introduction to Bioceramics,* L. L. Hench and J. Wilson (eds.), World Scientific Publishers, London and Singapore, 1993, p. 332.
10. G. LaTorre and L. L. Hench, "Analysis of bioactive glass interfacial reactions using Fourier-transform infrared reflection spectroscopy," in *Handbook on Characterization Techniques for the Solid–Solution Interface,* J. H. Adair, J. A. Casey, and S. Venigalla (eds.), American Ceramic Soc., Westerville, OH, 1993, pp. 177–195.

11. M. R. Filgueiras, G. P. LaTorre, and L. L. Hench, "Solution effects on the surface reactions of three bioactive glass compositions," *J. Biomed. Mater. Res.*, **27,** 1485–1493 (1993).
12. O. Sakamoto and S. Ito, "Mechanical properties of bioactive glass-ceramic reinforced by SiC whiskers," in *Handbook on Bioactive Ceramics, Vol. I,* T. Yamamuro, L. L. Hench, and J. Wilson (eds.), CRC Press, Boca Raton, FL, 1990, pp. 155–160.
13. T. Kasuga, K. Nakajima, T. Uno, and M. Yoshida, "Bioactive glass-ceramic composite toughened by tetragonal zirconia," in *Handbook on Bioactive Ceramics, Vol. 1,* T. Yamamuro, L. L. Hench, and J. Wilson (eds.), CRC Press, Boca Raton, FL, 1990, pp. 137–142.

Received May 17, 1995
Accepted August 3, 1995